

Novel Biodegradable Adaptive Hydrogels: Controlled Synthesis and Full Characterization of the Amphiphilic Co-Networks

Laetitia Mespouille,^[a] Olivier Coulembier,^[a] Dilyana Paneva,^[b] Philippe Degée,^[a] Iliya Rashkov,^[b] and Philippe Dubois*^[a]

Abstract: Adaptive and amphiphilic poly(*N,N*-dimethylamino-2-ethyl methacrylate-graft-poly[ϵ -caprolactone]) co-networks (*netP*(DMAEMA-*g*-PCL)) were synthesized from a combination of controlled polymerization techniques. Firstly, PCL cross-linkers were produced by ring-opening polymerization (ROP) of ϵ -CL initiated by 1,4-butane-diol and catalyzed by tin(II) 2-ethylhexanoate ([Sn(Oct)₂]), followed by the quantitative esterification reaction of terminal hydroxyl end-groups with methacrylic anhydride. Then, PCL cross-linkers were copolymerized to DMAEMA monomers by atom-transfer radical polymerization (ATRP) in THF at 60 °C using CuBr complexed by

1,1,4,7,10,10-hexamethyltriethylenetetramine (HMTETA) and 2-ethyl isobutyrylbromide (*Ei*BBBr) as catalytic complex and initiator, respectively. A comprehensive study of gel formation was carried out by employing dynamic light scattering (DLS) to determine the gel point as a function of several parameters and to characterize the viscous solutions obtained before the gel point was reached. The evolution of the mean diameters was compared to a

model previously developed by Fukuda and these attest to the living formation of the polymer co-network. Furthermore, we also demonstrated the reliability of ATRP for producing well-defined and homogeneous polymer co-networks by the smaller deviation from Flory's theory in terms of cross-linking density. For sake of clarity, the impact of polymerization techniques over the final structure and, therefore, properties was highlighted by comparing two samples of similar composition, but that were produced by either ATRP or thermal-initiated free-radical polymerization (FRP).

Keywords: atom-transfer radical polymerization (ATRP) • caprolactone • co-network • ring-opening polymerization

Introduction

Since the pioneering work of Wichterle and Lim in 1960 on cross-linked poly(2-hydroxyethyl) methacrylate (PHEMA),^[1] hydrogels have become a topic of great interest for biomedical^[2] and pharmaceutical^[3] applications, mainly due to their enhanced hydrophilic character and potential to be biocompatible. More recently, stimuli-respon-

sive hydrogels, also called "intelligent" hydrogels, have attracted much attention because of their capability to undergo relatively large and abrupt physical or chemical changes in response to small, external stimuli in their environmental media (e.g., pH, temperature, ionic strength, osmotic pressure),^[4,5] allowing their use in drug-delivery^[6] and tissue-engineering systems.^[7,8] To date, the most commonly used method to prepare cross-linked polymer networks is the free-radical polymerization (FRP) of vinyl and divinyl monomers.^[9–11] FRP has many advantages over other mechanisms, such as mild reaction conditions, tolerance to protic impurities such as water, and it is applicable to a wide range of monomers. Unfortunately, traditional FRP proceeds in a highly nonideal fashion with a large discrepancy with respect to the mean-field theory of Flory and Stockmayer (FS theory).^[12–16] As a consequence, there is no control over the network architecture and molecular parameters such as the molecular weight and polydispersity of chains between two cross-linking points, the cross-linker density, and volume distribution. This lack of control results in poorly defined ma-

[a] Dr. L. Mespouille, Dr. O. Coulembier, Dr. P. Degée, Prof. P. Dubois
Center of Innovation and Research in Materials and Polymers (CIRMAP)
Laboratory of Polymeric and Composite Materials
University of Mons-Hainaut 20, Place du Parc
7000 Mons (Belgium)
Fax: (+32)653-73-482
E-mail: philippe.dubois@umh.ac.be

[b] Dr. D. Paneva, Prof. I. Rashkov
Laboratory of Bioactive Polymers, Institute of Polymers
Bulgarian Academy of Sciences, 1113 Sofia (Bulgaria)

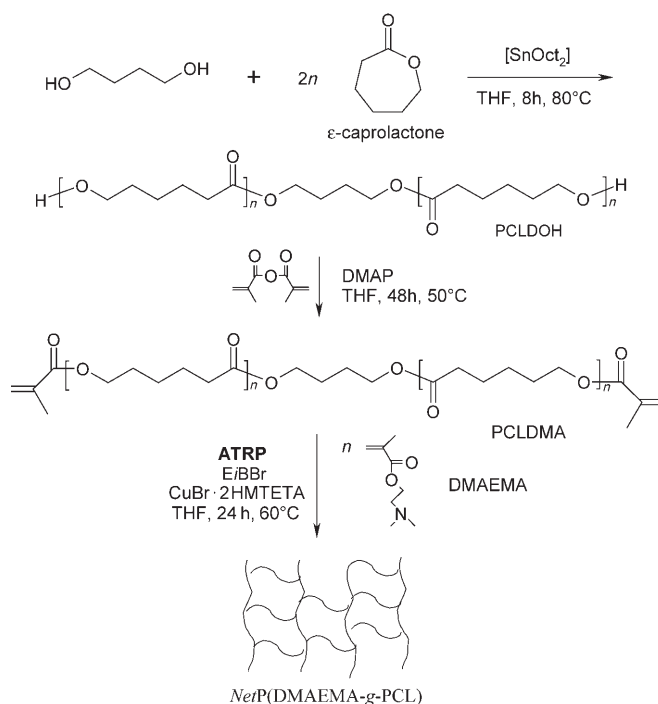
terials and increases the difficulty in correlating network structure to final properties of the gel.

In contrast, controlled radical polymerization (CRP) has emerged as a promising synthetic approach to producing high-performance materials. CRP is characterized by the occurrence of some reversible termination reactions between the growing polymer radical and a deactivation agent, which globally reduces the concentration of “active” radical species in favor of “dormant” ones. Consequently, the synthesis of well-defined polymers, including cross-linked structures, such as polymer hydrogels, is made possible. Ide and Fukuda^[17] took advantage of nitroxide-mediated polymerization (NMP) for the copolymerization of styrene with 4,4'-divinylphenyl (DVB) by using an oligomeric polystyryl adduct end-capped by 2,2,6,6-tetramethylpiperidinyl-1-oxyl as initiator. As a result, highly homogeneous hydrogels could be isolated with the critical cross-linking density that agrees with the FS theory. Liu et al.^[18] explored the possibility to exploit the reversible addition-fragmentation chain-transfer (RAFT) for the preparation of comb-type grafted poly[N-isopropylacrylamide-*g*-poly(N-isopropylacrylamide)] (P(NIPAM-*g*-PNIPAM)) and PNIPAM-*g*-poly(acrylic acid) (P(NIPAM-*g*-PAAc)) hydrogels. More recently, atom-transfer radical polymerization (ATRP) has also been used for the synthesis of cross-linked polymers. Jiang et al. reported a one-step gelation process involving the ATRP of either *N,N*-dimethylamino-2-ethyl methacrylate (DMAEMA) with ethyleneglycol dimethacrylate (EGDMA) cross-linker,^[19] or methyl methacrylate (MMA) with EGDMA^[20] for which they evidenced an autoacceleration rate at high conversion due to diffusion-controlled radical deactivation. Zhu et al.^[21,22] demonstrated that ATRP leads to more homogeneous networks than those produced by FRP.

Beyond the control over the molecular parameters and gel morphology, biodegradation is considered to be another key parameter in designing hydrogels for biomedical purposes with time-limited applications. In this respect, aliphatic polyester-based cross-linked hydrogels represent a class of degradable materials that meet these requirements. Furthermore, the introduction of hydrophobic segments is known to be beneficial to reinforce the mechanical properties of the swollen networks.^[23]

Here, we report on the controlled synthesis of amphiphilic *netP*[*N,N*-dimethylamino-2-ethyl methacrylate-*g*-poly(ϵ -caprolactone)] *netP*(DMAEMA-*g*-PCL) hydrogels through the combination of ring-opening polymerization (ROP) and atom-transfer radical polymerization (ATRP). To the best of our knowledge, such amphiphilic co-networks made of pH- and temperature-sensitive water-soluble poly(aminoalkylmethacrylate) segments and biodegradable aliphatic polyester cross-linkers has not yet been investigated. Practically, the synthesis of α,ω -methacrylate poly(ϵ -caprolactone) (PCLDMA) dimacromonomer was carried out by initiating the controlled ROP of ϵ -caprolactone (CL) by 1,4-butanediol in the presence tin(II) 2-ethylhexanoate ([Sn(Oct)₂]), followed by the quantitative esterification of the hydroxyl end-groups by methacrylic anhydride. Then, PCLDMA was

copolymerized with DMAEMA by ATRP in THF at 60 °C using CuBr ligated with 1,1,4,7,10,10-hexamethyltriethylenetetramine (HMTETA) and ethyl 2-bromoisobutyrate (*Ei*BBr) as catalyst and initiator, respectively (Scheme 1). For the sake of comparison, the synthesis of *netP*(DMAEMA-*g*-PCL) hydrogels was also carried out by free-radical polymerization (FRP) using azobis(isobutyronitrile) (AIBN) as initiator in THF at 60 °C. The as-formed hydrogels were thoroughly characterized in order to shed some light on the relations existing between the hydrogel properties and the synthesis method. As an example, we took advantage of the selective hydrolytic degradation of the polyester cross-linkers to determine the molecular weight and the polydispersity index of the remaining soluble and hydrophilic PDMAEMA segments.



Scheme 1. Three-step synthesis of poly[*N,N*-dimethylamino-2-ethyl methacrylate-*g*-poly(ϵ -caprolactone)] co-networks (*netP*(DMAEMA-*g*-PCL)).

Results and Discussion

α,ω -Hydroxy poly(ϵ -caprolactone)s (PCL(OH)₂) of various molar masses were obtained by ring-opening polymerization (ROP) of ϵ -caprolactone (CL) initiated by 1,4-butanediol (Bu(OH)₂) and catalyzed by tin(II) bis-2-ethyl hexanoate ([Sn(Oct)₂]) for a typical initiator-to-catalyst [Bu(OH)₂]₀/[Sn] molar ratio of 400, which prevents or at least hinders transesterification reactions.^[24] [Sn(Oct)₂] has been reported to react with hydroxyl groups through the fast and reversible formation of tin(II) alkoxide initiating species.^[25,26] Practically, CL polymerizations were carried out in THF at 80 °C for initial [CL]₀/[Bu(OH)₂]₀ molar ratios ranging from 15 to 50, then after a given polymerization time, terminated by

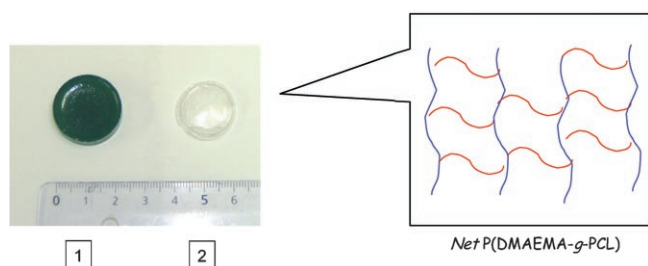


Figure 2. Optical images of *netP(DMAEMA-g-PCL)* samples as produced by ATRP before (1) and after (2) purification by immersion in a $\text{H}_2\text{O}/\text{THF}$ (1:1 by volume) mixture.

tallize in micrometric domains, at least for weight contents lower than 38% (Figure 2). Such behavior was confirmed by differential scanning calorimetry (DSC) in which thermograms did not exhibit any melting endotherm related to PCL segments (Figure 3). Therefore, the copolymerization of hydrophilic DMAEMA with hydrophobic PCLDMA cross-linker by ATRP in THF at 60°C results in the formation of amphiphilic polymer co-networks with high yield and non-crystalline PCL nanodomains randomly dispersed.

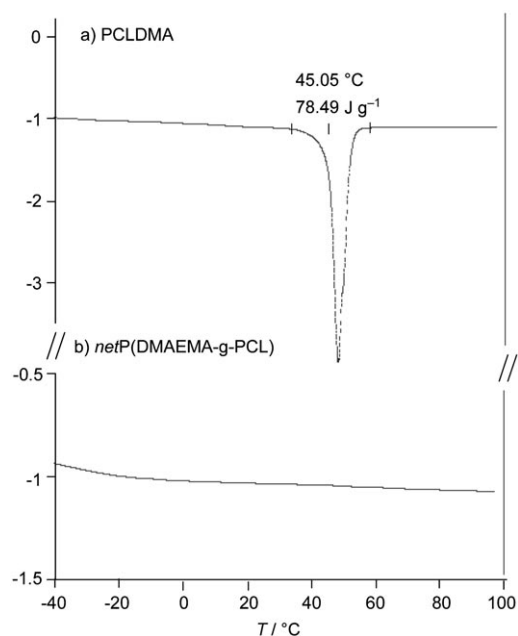


Figure 3. DSC thermograms of a) PCLDMA ($M_n=3100\text{ g mol}^{-1}$) and b) *netP(DMAEMA-g-PCL)* (entry 2, Table 1) (2nd scan, $10^\circ\text{C min}^{-1}$ from -40 to $+100^\circ\text{C}$, under nitrogen).

In addition to gravimetry measurements giving access to the weight fraction in PCLDMA and the gel fraction of co-networks prepared by ATRP, elementary analysis was carried out in triplicates. From the relative nitrogen content, the actual experimental molar fraction in DMAEMA units (F_n^{DMAEMA}) could be calculated for the three polymer co-networks (Table 1). Interestingly, DMAEMA composi-

tions in the feed and final co-networks were very similar, indicating that co-monomer conversion was close to completion under the prevailing experimental conditions. This gives credit to the reliability of the gel fraction as evidence of co-network formation and demonstrates that most of the extracted molecules consist of non-cross-linked graft copolymers rather than unreacted monomers.

Table 1. Molecular-weight characteristics of *netP(DMAEMA-g-PCL)* samples as obtained by ATRP in THF at 60°C initiated by EiBBR and catalyzed by $\text{CuBr}\cdot 2\text{HMTETA}$ for an initial co-monomer concentration of 4.8 mol L^{-1} and an initial molar fraction (F_n^{PCLDMA}) of 3%.

Entry	M_n^{PCLDMA} [g mol^{-1}] ^[a]	F_w^{PCLDMA} [%] ^[b]	F_G [%] ^[c]	F_n^{DMAEMA} [%] ^[d]	F_n^{DMAEMA} [%] ^[e]
1	1700	25.3	90	97	97.45 ± 0.14
2	3100	37.9	94	97	96.25 ± 0.02
3	3100	37.9	90	97	95.74 ± 0.06

[a] Number-average molecular weight of PCLDMA as calculated by $^1\text{H NMR}$. [b] Initial weight fraction of PCL in the feed. [c] F_G = gel fraction obtained after elimination of residual catalyst, unreacted co-monomers and any non-cross-linked graft copolymers by using the following equation: $F_G = w_g/w_p$, in which w_g and w_p represent the weight of the dried sol-free network sample after solvent evaporation under reduced pressure, and the total weight of co-monomer introduced, respectively. [d] Initial molar fraction in DMAEMA subunits as determined by the following relationship: $F_n^{\text{DMAEMA}} = n^{\text{DMAEMA}}/(n^{\text{DMAEMA}} + n^{\text{CL}})$ in which n^{DMAEMA} and n^{CL} are the mole number of DMAEMA and CL subunits in the feed, respectively. [e] Experimental molar fraction in DMAEMA units as determined by N-elementary analysis.

According to Flory's theory,^[28] the gel point can be defined as the time required to reach an abrupt transition from a viscous liquid made of individual polymer chains to an elastic gel. It can also be seen as the reaction time above which small cross-linked domains merge to form a single swollen polymer network, also called "critical gel".^[29] In this work, the determination of the gel point is a key parameter in the comprehensive study of gel formation. The gel point was first determined as a function of both the initial co-monomer concentration ($[\text{DMAEMA} + \text{PCLDMA}]_0$) and M_n^{PCLDMA} , by using the *tube-inversion method*. Practically, *netP(DMAEMA-g-PCL)* polymer co-networks were synthesized by ATRP as aforementioned for concentrations in co-monomers ranging from 2 to 4.8 mol L^{-1} and M_n^{PCLDMA} of 4300 and 5800 g mol^{-1} . The initial PCLDMA molar composition was kept at 3%. Samples were periodically withdrawn from the oven at 60°C and the reaction was quenched by cooling the mixture in an ice-bath. Figure 4 shows the effect of initial concentration in co-monomers and PCLDMA molar mass on the *gel point*. As might be expected, increasing the concentration in co-monomers from 2 to 4.8 mol L^{-1} enhances the kinetics, especially for concentrations of 2 to 3 mol^{-1} .

Furthermore, the increase in the PCLDMA molecular weight from 4300 to 5800 g mol^{-1} does not influence significantly the gel point, at least, at low co-monomer concentrations, attesting that polymer chain length is not a major parameter in modulating gel-point apparition.

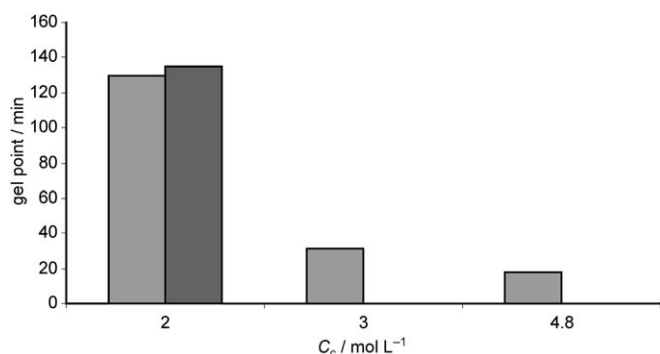


Figure 4. Impact of the initial co-monomer concentration C_c ($[\text{DMAEMA}]_0 + [\text{PCLDMA}]_0$) and PCLDMA molecular weight on the gel point; ■: $M_n = 4300 \text{ g mol}^{-1}$; ▨: $M_n = 5800 \text{ g mol}^{-1}$.

In a second series of experiments, the kinetics of gel formation was further investigated by limiting the degree of conversion below the gel point and using dynamic light scattering (DLS) as a tool to estimate the average diameter of the structures formed as a function of time. The copolymerization of DMAEMA and PCLDMA was carried out by ATRP for an initial co-monomer concentration of 2 mol L^{-1} , $M_n \text{PCLDMA} = 4300 \text{ g mol}^{-1}$, and a reaction time of less than 2 h. The resulting viscous crude products were added with a minimum volume of THF before precipitation from cold heptane. The precipitates were recovered by filtration, dried under reduced pressure, and extracted with a THF/ H_2O (1:1 by volume) mixture for 48 h. The purified polymer networks were then characterized by DLS in THF for a concentration of 1 g L^{-1} .

For each sample, quite broad and monomodal nanosized species distributions were evidenced and their average mean diameter estimated by the non-negative least-squares (NNLS) deconvolution method. Based on the models reported by Fukuda et al.^[30] describing gel formation by either conventional or “living” radical polymerization (Figure 5), a smoother time dependence of the hydrodynamic volume of polymer structures can be expected for “living” radical polymerization before reaching the gel point. This can be explained by the lower concentration in radical species promoting fewer intramolecular cross-linking reactions and decreasing the extent of microgels formation. Whatever the radical mechanism, the hydrodynamic volume increases sharply close to the gel point. Figure 6 shows that the mean diameter remains very low before the gel point, which might

be in agreement with Fukuda’s model. However, such an assumption needs further experimental data to be confirmed.

Interestingly, further investigations were performed by ^1H NMR spectroscopy on the residual sol fractions (=soluble fractions) obtained after 0.5, 1, 2, 3, and 4 h of copolymerization reaction ($[\text{DMAEMA}]_0 + [\text{PCLDMA}]_0 = 4.8 \text{ mol L}^{-1}$). These demonstrated a constant concentration of carbon–carbon double bonds remaining in the reaction medium. This last result is in good accordance with the monotonous addition of monomers over time as expected for a “living” process. This confirms that hydrogels produced by ATRP do not result from the association of previously generated microgels.

As might be expected, the initial cross-linker molar fraction ($F_n \text{PCLDMA}$) is another key parameter influencing the

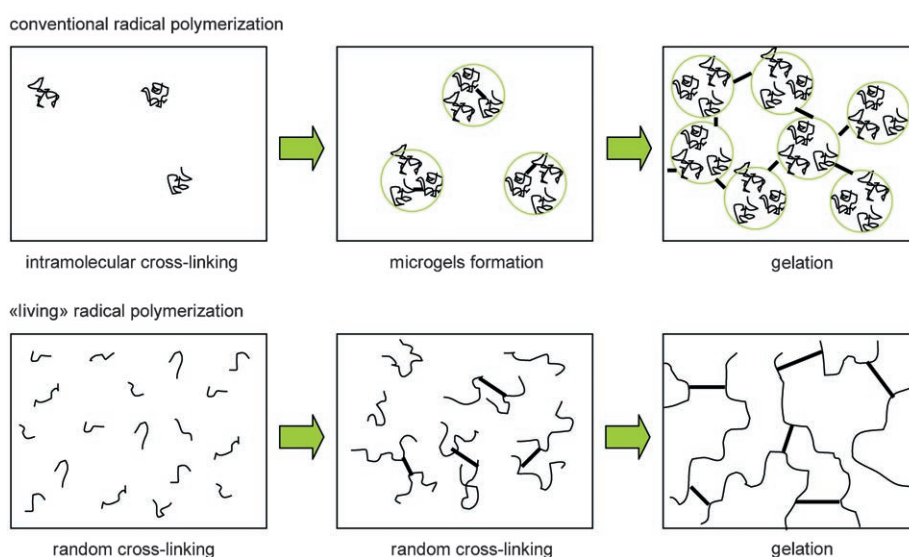


Figure 5. Schematic representation of the assumed cross-linking reactions in conventional and “living” radical polymerizations, as redrawn from reference [30].

gel point. Figure 7 depicts the dependence of the gel point on the PCLDMA molar fraction in the feed for $M_n \text{PCLDMA} = 4300 \text{ g mol}^{-1}$ and $[\text{DMAEMA}]_0 +$

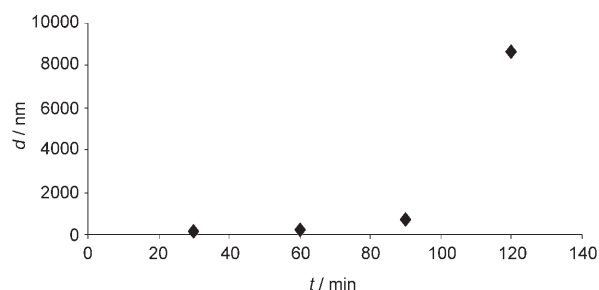


Figure 6. Time dependence of the mean diameter of the growing polymer nanogels formed by ATRP as determined by DLS for a 1 g L^{-1} copolymer solution in THF at RT.

$[PCLDMA]_0 = 4.8 \text{ mol L}^{-1}$. Increasing F_n PCLDMA fraction from 3 to 6% decreases the time required for gel formation.

Understandably, the gel growth is not only caused by chain-growth propagation of (co)monomers, but also by in-

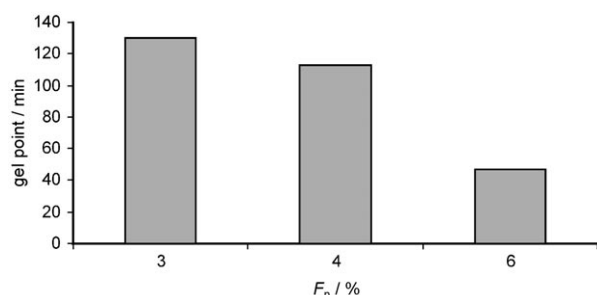


Figure 7. Plot of gel point vs. initial molar fraction in PCLDMA (F_n PCLDMA).

corporation of sol polymers through reactions between radicals and pendant double bonds of both gel and sol populations. Upon this basis, and knowing the prevailing insertion of PCLDMA cross-linker into the network structure compared to DMAEMA monomer, increasing the PCLDMA fraction and, therefore, the amount of pendant double bonds contribute to a more rapid gelation of the reactive medium.

As amply described in the literature, the final co-network structure tremendously affects the swelling rate and equilibrium degree of swelling (S_{eq}) and vice versa. To gather further evidence that the polymerization mechanism influences the co-network structure, two polymer co-networks were prepared, respectively, by ATRP (entry 3, Table 1) and FRP for a similar feed composition, and their swelling properties were investigated in Millipore water. Practically, DMAEMA and PCLDMA ($M_n = 3100 \text{ g mol}^{-1}$, $PDI = 1.14$) were copolymerized in THF at 60°C either by conventional radical polymerization using azobisisobutyronitrile (AIBN) as initiator ($[DMAEMA]_0 + [PCLDMA]_0/[AIBN]_0 = 200$) for 24 h or by ATRP according to previously mentioned experimental conditions. The initial molar fraction in PCLDMA was fixed at 3% and the co-monomer concentration was 4.8 mol L^{-1} . After the copolymerization reaction under inert atmosphere, the polymer co-networks were recovered from the glass vials and the soluble unreacted fraction was extracted by immersion/diffusion in a THF/ H_2O mixture (1:1 by volume). Table 2 shows the initial and final compositions of polymer networks prepared by ATRP and FRP, respectively. It is apparent that feed and polymer network compositions are very similar to each other, as determined by N-elementary analysis, whereas the gel fraction by conventional radical polymerization is somehow higher than for ATRP.

Upon immersion in deionized water at 20°C , the polymer co-networks swell and the time dependence of water uptake was determined by blotting each slab of swollen networks and weighing. The swelling ratio (S) of hydrogels is defined in Equation (1) as:

Table 2. Gel fraction, initial, and final compositions of the polymer networks prepared by both ATRP and FRP.

Entry	Mechanism	F_n DMAEMA [%] ^[a]	F_n DMAEMA [%] ^[b]	F_G [%] ^[c]
3	ATRP	97	95.74 ± 0.06	90
4	FRP	97	97.04 ± 0.01	97

[a] Initial molar fraction in DMAEMA. [b] Experimental molar fraction in DMAEMA subunits as determined by N-elementary analysis. [c] Gel fraction as determined after purification of polymer co-networks according to the following equation: $F_G = 100 \times w_g/w_p$ in which w_g and w_p denote the weight of the dried sol-free network and the total co-monomer weight in the feed, respectively.

$$S = (m_w - m_d)/m_d \quad (1)$$

in which m_d and m_w are the masses of dry and swollen polymer network, respectively, at a given time. The average values of three measurements were plotted against time until equilibrium was reached (S_{eq}).

Figure 8 compares the swelling behavior of hydrogels obtained by ATRP (■) and FRP (□). Interestingly, the degree of swelling at equilibrium (S_{eq}) of the gel produced by FRP is half of that of the gel produced by ATRP, indicating that different network structures are formed as a function of the polymerization mechanism. In ATRP, the fast activation/deactivation equilibrium is shifted towards dormant species so that the concentration of active growing radical is reduced, as well as the propagation rate. It often takes hours for an individual chain to add hundreds of monomers, whereas this time is reduced to few second in FRP. Such a high propagation rate and poor chain relaxation are responsible for the formation of heterogeneous networks with highly cross-linked microdomains and extra macromolecular entanglements restricting chain mobility and swelling.^[19]

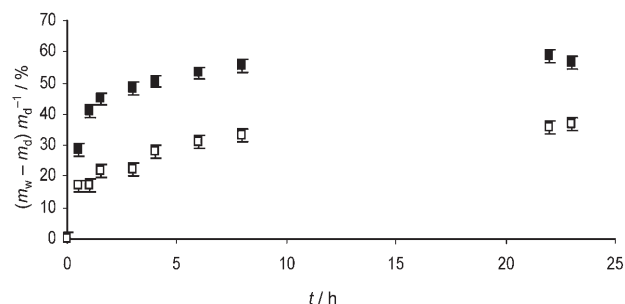
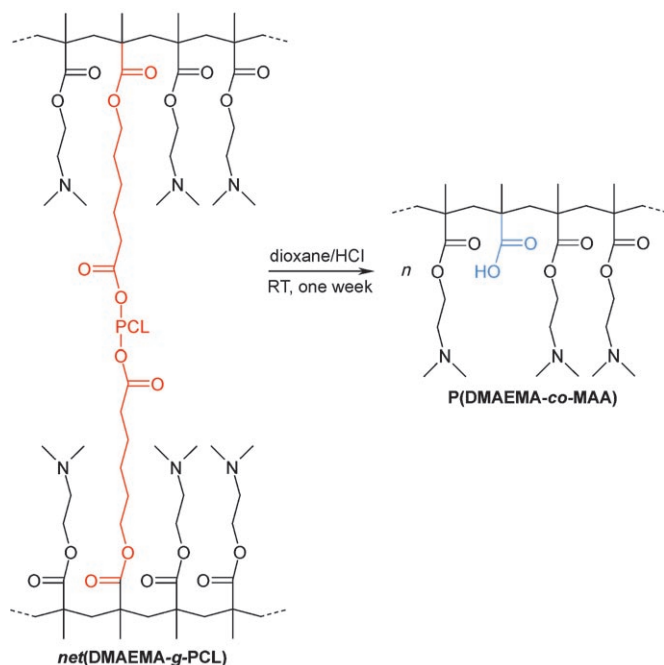


Figure 8. Time dependence of swelling ratio in deionized water at RT for *netP*(DMAEMA-*g*-PCL) polymer networks as produced by ATRP (■, $S_{eq} = 55\%$) and FRP (□, $S_{eq} = 35\%$).

In contrast to the FRP process, the ATRP mechanism is known to allow the synthesis of linear polymer chain with controlled molecular weight and narrow polydispersity index. In the context of this research, it was of great interest to evaluate the influence of such a “living”/controlled mechanism on the cross-linking reaction and more particularly, on the polymethacrylate backbone. For this purpose, the polyester cross-linkers were selectively hydrolyzed in a diox-

ane/aqueous HCl mixture (85:15 by volume) at room temperature for one week (Scheme 2). The results of this hydrolysis are the release of hydroxycaproic acid and the formation of free poly(*N,N*-dimethylamino-2-ethyl methacrylate-*co*-methacrylic acid) (P(DMAEMA-*co*-MAA)).

After one week degradation time, the solvent mixture was evaporated under vacuum and replaced by Millipore water.



Scheme 2. Selective hydrolysis of PCLDMA cross-linkers from *net*P(DMAEMA-*g*-PCL) polymer co-networks.

The pH was increased to 9 by adding NaOH aqueous solution to restore amino pendant groups, and the polymethacrylate backbones were precipitated out by heating the aqueous solution up to 60 °C, taking advantage of the lower critical solution temperature (LCST) of PDMAEMA-based polymers.^[31] The ¹H NMR spectrum of the precipitate in CDCl₃ attests to the high selectivity of the hydrolysis towards PCL cross-linkers, as confirmed by the selective presence of protons corresponding to poly(*N,N*-dimethylamino-2-ethyl methacrylate-*co*-methacrylic acid) polymer chains (P(DMAEMA-*co*-MAA)). In other words, the ester functions of DMAEMA subunits are preserved. This ob-

servation is further confirmed by the good accordance between the $I_c/I_d/I_e$ ratio and the theoretical 2:2:6 ratio, at least within the inherent ¹H NMR experimental errors (Figure 9).

Note that no discrimination could be observed by SEC for a preformed PDMAEMA homopolymer before and after submission to similar hydrolysis conditions, although this technique has already demonstrated its effectiveness.^[32] Therefore, it can be assumed that hydrolysis is highly selective towards PCL cross-linkers.

SEC analyses were carried out on the hydrolysis products issued from polymer co-networks produced by ATRP and FRP. A narrower polydispersity for polymethacrylate backbone is produced by ATRP ($M_w/M_n=2$), relative to conventional radical polymerization ($M_w/M_n=4.5$). Furthermore, the apparent molecular weight of the resulting P(DMAEMA-*co*-MAA) obtained by ATRP ($M_{napp}=16000\text{ g mol}^{-1}$) is at the same order of magnitude as a PDMAEMA with a targeted DP (DP=degree of polymerization) of 100, which may give credit to some control over molecular parameters in the polymer co-network. In contrast, P(DMAEMA-*co*-MAA) derived from the FRP process is characterized by a much higher apparent molecular weight ($M_{napp}=50000\text{ g mol}^{-1}$, theoretical DP=2- $([DMAEMA]_0 + [PCLDMA]_0)/[AIBN]_0=100$).

So far it has been demonstrated that ATRP represents a very convenient method to produce homogeneous and well-defined polymer networks. However, no information is available on the occurrence of side reactions and on the presence of such defects as loops or pendant double bonds, which deviate from the ideal model developed by Flory.^[28] In Flory's model, gelation occurs at the point at which, on an average basis, each primary chain contains one cross-link-

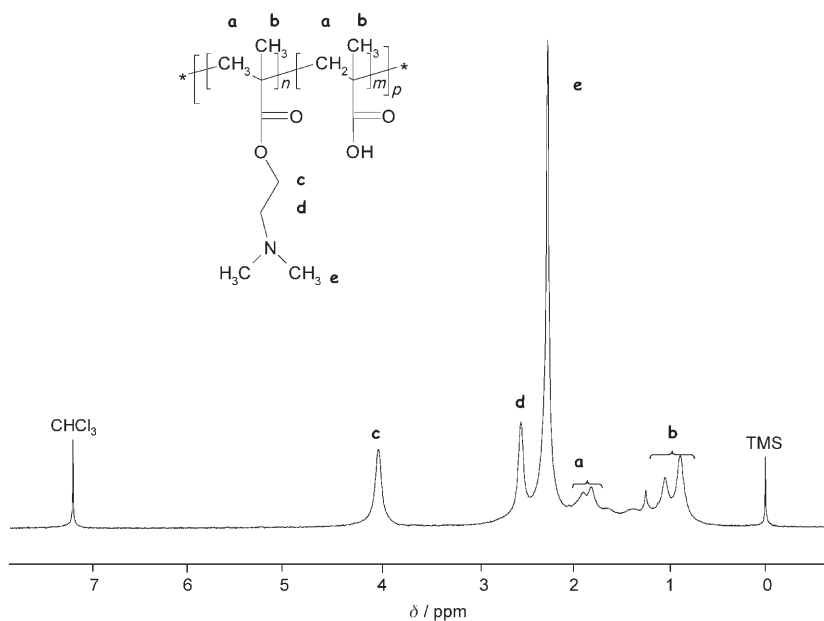


Figure 9. ¹H NMR spectrum measured in CDCl₃ of P(DMAEMA-*co*-MAA) backbone resulting from the selective degradation of PCLDMA cross-linker in a dioxane/HCl mixture.

ing point, resulting in an homogeneous network, which is a network statistically assembled from equally reactive vinyl groups and exempt of defects. To quantify the number of defects in the polymer networks prepared by ATRP, the cross-linking density was calculated by the Charlesby and Pinner relationship [Eq. (2)]:^[33]

$$s + s^{1/2} = (\rho r_{np})^{-1} \quad (2)$$

in which s is the sol fraction ($s = 1 - F_G$), ρ is the cross-linking density, and r_{np} is the average number of primary chain length.

For a “living”/controlled polymerization such as ATRP, r_{np} can be predicted from the initial monomer-to-initiator ratio corrected by the monomer conversion, $r_{np} = [M]_0 \text{ conv.} / [I]_0$ (in this work $[M]_0/[I]_0 = 100$). By plotting $s + s^{1/2}$ versus $1/\text{conversion}$, the slope gives access to the cross-linking density (ρ).

Practically, the copolymerization of PCLDMA ($M_n = 3100 \text{ g mol}^{-1}$, $M_w/M_n = 1.14$) and DMAEMA was initiated by EiBBBr and catalyzed by $\text{CuBr} \cdot 2\text{HMTETA}$ in THF at 60°C for an initial co-monomer-to-initiator molar ratio of 100. The initial molar fraction in PCLDMA and initial co-monomer $[\text{PCLDMA}]_0 + [\text{DMAEMA}]_0$ concentration were fixed to 3% and 4.8 mol L^{-1} , respectively. The copolymerizations were quenched at 0°C for reaction times ranging from 0.5 to 4 h and the unreacted soluble fractions were extracted by immersion/diffusion in a $\text{H}_2\text{O}/\text{THF}$ solvent mixture (1:1 by volume) in the presence of methylether benzoquinone to inhibit any radical reactions.

The cross-linking density ρ was calculated from the plot in Figure 10 and equals 0.026, which is very close to the value of 0.029 determined by Hunkeler et al.^[19] for

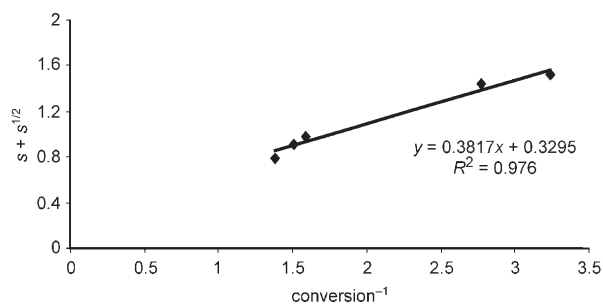


Figure 10. Determination of the cross-linking density from the plot of $s + s^{1/2}$ vs. $1/\text{conv.}$

PDMAEMA-based networks prepared by ATRP using ethylene glycol dimethacrylate as cross-linking agent. Notably, these values differ only by a factor of three compared to Flory’s equation ($\rho = 0.01$), which is quite satisfying taking into account the difference of several orders of magnitude usually observed for conventional FRP. In other words,

ATRP cannot avoid the presence of intramolecular cyclization and trapping of pendant double bonds, but the content of such defects is much smaller than in the case of conventional FRP.

The impact of the control of the polymerization process on the structure of the resulting co-networks was evidenced by the previously discussed swelling investigation and further reinforced by the good accordance of the cross-linking density of the gel produced by ATRP to Flory’s theory. This impact can be further highlighted by direct observation of the gel morphology by scanning electron microscopy (SEM). For this purpose, pieces of gel produced by either FRP or ATRP (Table 2) were immersed in aqueous HCl (pH 3) until equilibrium was reached, and then freeze-dried. Figure 11 presents the SEM micrographs of the respective

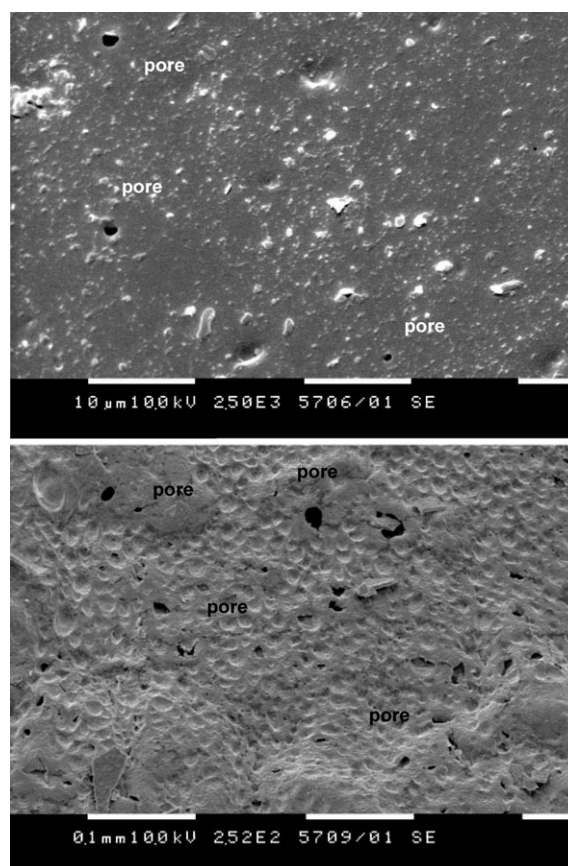


Figure 11. SEM micrographs of freeze-dried $\text{netP(DMAEMA-g-PCL)}$ co-networks produced by top) FRP and bottom) ATRP (see Table 2).

freeze-dried samples. Surprisingly, the gel produced by FRP is quite smooth and only punctual pores were detected (average diameter = $1.3 \mu\text{m}$). In contrast, the gel obtained by ATRP presents a quite rough and organized surface composed mostly of “alveoli” of identical size (Figure 12). Although few pores can be observed (average diameter = $13 \mu\text{m}$) in the image, this surface organization tends to indicate that pores remain essentially inside the polymer network.

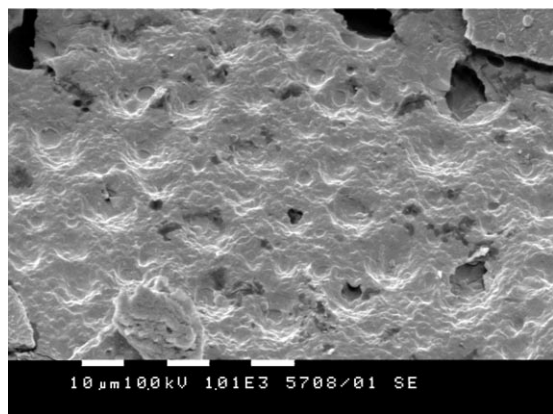


Figure 12. SEM micrograph showing “alveoli” present at the surface of the ATRP co-network (see Table 2).

Conclusion

The copolymerization of DMAEMA and PCLDMA by ATRP allows for the preparation of homogeneous amphiphilic *netP*(DMAEMA-*g*-PCL) polymer co-networks with large gel fractions ($90 \leq F_G \leq 95\%$) and compositions very close to the feed, as determined by N-elementary analysis. Their purification by immersion/diffusion in a THF/H₂O solvent mixture (1:1 by volume) is very efficient and leads to colorless gels. A study of the gel formation attests for the dependence of the gel point on the initial co-monomer concentration, the PCLDMA cross-linker molar fraction, and molar mass. Investigations performed on the viscous solutions obtained before reaching the gel point show that the co-network formation by ATRP proceeds slower than by FRP, although the former method yields a more homogeneous network, preventing the self-assembly of microgels. As might be expected, the polymerization mechanism affects the polymer structure and swelling behavior in water, as well as molecular weight of the polyester chains between cross-linking. For instance, the actual molar mass is closer to the targeted one and molar-mass distributions are narrower, as determined by SEC after selective hydrolysis of PCL cross-linkers. In other words, the mesh size of the polymer co-networks becomes predictable. Last but not least, in contrast to the FRP mechanism, hydrogels produced by ATRP show smaller deviations from Flory's theory in term of cross-linking density, which may be ascribed to fewer defects such as loop formation or dangling ends. SEM analysis confirms clearly the difference in gel morphology; a smooth surface was observed for the gel produced by FRP whereas an organized surface presenting alveoli was observed for the gel obtained by ATRP. The adaptive properties of the resulting *netP*(DMAEMA-*g*-PCL) co-networks have been studied as a function of the medium pH and temperature. These results will be published in a forthcoming paper.

Experimental Section

Materials and methods: ϵ -Caprolactone (CL) (Acros, 99%) was dried over calcium hydride at RT for 48 h and then distilled under reduced pressure. *N,N*-dimethylamino-2-ethyl methacrylate (DMAEMA) (Aldrich, 98%) was deprived of its inhibitor by filtration through a basic alumina column. 1,4-Butane-diol (Acros, > 99%) was dried over calcium hydride at RT for 48 h and distilled at 70 °C under reduced pressure. Triethylamine (NEt₃, Fluka, 99%) was dried over barium oxide at RT for 48 h and distilled under reduced pressure. Copper bromide (CuBr, Fluka, 98%) was purified in acetic acid and recrystallized in ethanol under inert atmosphere until a white powder was obtained. Bis(2-ethyl hexanoate)tin ([Sn(Oct)₂], Aldrich, 95%), methacrylic anhydride (Aldrich, 94%), *N,N*-dimethylamino-4-pyridine (DMAP, Acros 99%), 1,1,4,7,10,10-hexamethyltriethylenetetramine (HMTETA, Aldrich, 97%), ethyl-2-bromoisobutyrate (EiBBR, Aldrich, 98%), and *N,N'*-dicyclohexylcarbodiimide (DCC, Acros, 99%) were used as received. Tetrahydrofuran (THF, Labscan, 99%) was dried over molecular sieves (4 Å) and distilled over polystyryl lithium (PS⁻Li⁺) under reduced pressure just before use. Toluene (Labscan, 99%) was dried by refluxing over CaH₂ and distilled just before use.

α,ω -Dihydroxy poly(ϵ -caprolactone) PCL(OH)₂ by ROP: In a previously dried and nitrogen-purged round-bottomed flask equipped with a three-way stopcock and a rubber septum, 20 mL (0.18 mol) of ϵ -caprolactone was added to 14 mL freshly dried THF. [Sn(Oct)₂] (1 mL, 0.09 mmol) in THF solution (0.09 mol L⁻¹) was added and the temperature was increased to 80 °C before adding 0.8 mL (0.009 mmol) of 1,4-butane-diol previously dried and distilled over CaH₂. After 8 h the reaction was stopped by adding dropwise aqueous HCl (1 mol L⁻¹) in slight excess with respect to catalyst content. The polymer was then selectively precipitated from a large volume of cold heptane, filtered and dried under reduced pressure until constant weight. Tin residues were removed by liquid/liquid extraction by washing the polyester solution in chloroform once with aqueous HCl and twice with water. Finally, the organic layer was poured into cold heptane to recover the α,ω -hydroxy-poly(ϵ -caprolactone) (PCL(OH)₂) by precipitation (yield > 99%).

Derivation of hydroxyl end-groups into methacrylate functions by esterification reaction: In a previously dried and nitrogen-purged round-bottomed flask was dissolved methacrylic anhydride (4.8 g, 31 mmol) in previously dried THF (100 mL). In another previously dried round-bottomed flask equipped with a three-way stopcock and a rubber septum flask, PCL(OH)₂ (15 g, 6.2 mmol, $M_n = 2400$ g mol⁻¹) and DMAP (0.31 g, 2.5 mmol) were previously dried by three consecutive toluene azeotropic distillations before adding dried THF (100 mL) and triethylamine (3.1 g, 31 mmol). This latter mixture was slowly added to the solution of methacrylic anhydride and the temperature was increased to 50 °C. After 48 h, the α,ω -methacrylate-poly(ϵ -caprolactone) (PCLDMA) was recovered by selective precipitation from a large volume of cold methanol, filtration, and drying under reduced pressure at 40 °C until constant weight (14.5 g, 96.8%). ¹H NMR (300 MHz, CDCl₃), Figure 1: $\delta = 1.3$ (m, 4H_s), 1.6 (m, 8H_d), 1.65 (m, 4H_a), 1.8 (s, 6H_e), 2.2 (t, 4H_c), 4.05 (t, 4H_f), 4.1 (t, 4H_b), 5.6 and 6.1 ppm (s, 1H_i + 1H_j).

Synthesis and purification of poly[*N,N*-dimethylamino-2-ethyl methacrylate-*g*-poly(ϵ -caprolactone)] networks *netP*(DMAEMA-*g*-PCL) by ATRP: CuBr (46.2 mg, 0.32 mmol) and 1,1,4,7,10,10-hexamethylenetetramine (148.4 g, 0.64 mmol) and a magnetic stirrer were introduced in open air into a round-bottomed flask, which was then closed by a three-way stopcock capped by a rubber septum and deprived of oxygen by three freezing/thawing cycles. Typically, PCLMA (3.478 g, 0.97 mmol, $M_n = 3600$ g mol⁻¹), THF (1.7 mL), and *N,N*-dimethylamino-2-ethyl methacrylate (5 mL, 31.2 mmol) were introduced into a dry, round-bottomed flask and bubbled with nitrogen before transferring the mixture onto the catalytic complex. Then, degassed ethyl 2-bromoisobutyrate (47.5 μ L, 0.32 mmol) was added to the reactive mixture under nitrogen flow and several 1-mL portions were separately distributed in previously dried and nitrogen-purged glass vials before being set into an oven thermostatted at 60 °C. After 24 h, polymer networks were isolated from their vials and introduced to a mixture of H₂O/THF (1:1 by volume) to extract the

copper catalyst and soluble fraction. Colorless samples were then dried under vacuum at RT until constant weight.

Selective hydrolytic degradation of polyester linkers in refluxing dioxane/HCl mixture: Hydrogel samples were introduced to an aqueous mixture of dioxane/37% HCl (17:1 by volume) at 30°C. After one week, gels were totally degraded resulting in a clear solution. The solvent was evaporated under vacuum and replaced by distilled water. The pH was raised to 9 by adding concentrated aqueous NaOH and the precipitation of the PDMAEMA chains was induced by increasing the temperature up to 80°C. The polymers were recovered by filtration and dried under vacuum at 40°C overnight until constant weight. Yield: 71.6%. ¹H NMR (300 MHz, CDCl₃, Figure 9): δ=0.8–1.2 (m, 3H_c), 1.7 (t, 3H_d), 1.8–2.0 (m, 2H_d + 6H_e), 2.3 (s, 6H_b), 2.5 (t, 2H_g), 4.0 ppm (t, 2H_f + 2H_i).

N-elemental analysis: The dynamic combustion of the samples was performed with a Flash EA112 Elemental Analysis equipped with an AS3000 autosampler and using the Eager 300 dedicated software (available at Carlo Erba Strumentazione directed by Dr. Giuzzi, Rodano, Milano, Italy). Nitrogen determination was based on the Kjeldahl method. Practically, N-elemental analysis was carried out in triplicate per sample and experimental molar fraction in DMAEMA units was determined from the following relationships:

$$F_{w,DMAEMA} = (F_{w,N}/M_{w,N}) \times M_{w,DMAEMA}$$

$$F_{w,PCLDMA} = 1 - F_{w,DMAEMA} \quad (3)$$

$$F_{n,DMAEMA} = (F_{w,DMAEMA}/M_{w,DMAEMA}) / [(F_{w,DMAEMA}/M_{w,DMAEMA}) + (F_{w,PCLDMA}/M_{w,PCLDMA})]$$

in which $F_{w,DMAEMA}$, $F_{w,N}$, $F_{w,PCLDMA}$ denote the experimental weight fraction in DMAEMA, nitrogen, and PCLDMA, respectively; $F_{n,DMAEMA}$ is the experimental molar fraction in DMAEMA, and $M_{w,N}$, $M_{w,DMAEMA}$, and $M_{w,PCLDMA}$ correspond to the molecular weights of nitrogen, DMAEMA, and PCLDMA, respectively.

Swelling experiments: Dry hydrogel slabs were immersed in Millipore water and withdrawn at determined time intervals, blotted with tissue paper to absorb excess surface water, and weighed. The swelling degree was determined at RT as a function of time by using the following relationship [Eq. (4)]:

$$S(\%) = (m_w - m_d) / m_d \quad (4)$$

in which m_w and m_d represent the mass of the wet and dry gel, respectively.

Characterizations: ¹H NMR spectra were recorded by using a Bruker AMX-300 or AMX-500 apparatus at RT in CDCl₃ (30 mg per 0.6 mL). Size exclusion chromatography (SEC) was performed in THF (poly(ε-caprolactone)) or THF + 2 wt % NEt₃ (DMAEMA containing copolymers) at 35°C by using a Polymer Laboratories liquid chromatograph equipped with a PL-DG802 degasser, an isocratic HPLC pump LC 1120 (flow rate=1 mL/min), a Marathon autosampler (loop volume=200 μL, solution concn=1 mg/mL), a PL-DRI refractive-index detector, and three columns: a PL gel 10-μm guard column and two PL gel Mixed-B 10-μm columns (linear columns for separation of MW_{PS} ranging from 500 to 10⁶ daltons). Poly(styrene) standards were used for calibration. Temperature (modulated) DSC measurements were performed under nitrogen flow by using a 2920CE DSC apparatus from TA Instruments (heating rate from 1–10°Cmin⁻¹, modulation amplitude of 1°C and period 60°C). Dynamic light scattering measurements were carried out using a BI-160 apparatus (Brookhaven Instruments Corporation, USA) with a He–Ne laser source operating at 17 mW and delivering a vertically polarized light (λ=633 nm). The particle sizes and size distribution were calculated using NNLS algorithms. The surfaces of the hydrogels were evaluated by scanning electron microscopy (SEM). For this purpose, preliminary freeze-dried swollen-to-equilibrium (pH 3, HCl aqueous solution) hydro-

gels were vacuum coated with carbon and gold and analyzed using a SEM Philips 515 (see Experimental Section).

Acknowledgements

L.P.C.M. is very grateful to “Région Wallonne” and the European Union (FEDER, FSE) for general financial support in the frame of Objectif 1-Hainaut: Materia Nova, as well as to the Belgian Federal Government Office of Science Policy (SSTC-PAI 6/23). L.M. and O.C. are a research fellow and post-doctoral researcher, respectively, of the Belgian F.N.R.S (Fonds National de la Recherche Scientifique). This work was partly supported by the Bulgarian National Fund for Scientific Research (Grant CH-1414).

- [1] O. Wichterle, D. Lim, *Nature* **1960**, *185*, 117.
- [2] A. S. Hoffman, *Adv. Drug Delivery Rev.* **2002**, *54*, 3.
- [3] N. A. Peppas, P. Bures, W. Leobandung, H. Ichikawa, *Eur. J. Pharm. Biopharm.* **2000**, *50*, 27.
- [4] B. Jeong, A. Gutowska, *Trends Biotechnol.* **2002**, *20*, 305.
- [5] A. Kikuchi, T. Okano, *Prog. Polym. Sci.* **2002**, *27*, 1165.
- [6] “Hydrogels”: M. A. Lowman, N. A. Peppas in *Encyclopaedia of Controlled Drug Delivery* (Ed.: E. Mathiowitz), Wiley, **1999**, pp. 397–418.
- [7] L. G. Cima, J. P. Vacanti, C. Vacanti, D. Ingber, D. Mooney, R. Langer, *J. Biomech. Eng.* **1991**, *113*, 143.
- [8] J. A. Hubbel, R. Langer, *Chem. Eng. News* **1995**, 42.
- [9] S. Zhu, A. E. Hamiliec, *Macromolecules* **1992**, *25*, 5457.
- [10] S. Zhu, A. E. Hamiliec, *Macromolecules* **1993**, *26*, 3131.
- [11] S. Zhu, *Macromolecules* **1996**, *29*, 456.
- [12] P. J. Flory, *J. Am. Chem. Soc.* **1941**, *63*, 3083.
- [13] P. J. Flory, *J. Am. Chem. Soc.* **1941**, *63*, 3091.
- [14] P. J. Flory, *J. Am. Chem. Soc.* **1941**, *63*, 3096.
- [15] W. H. Stockmayer, *J. Chem. Phys.* **1943**, *11*, 45.
- [16] W. H. Stockmayer, *J. Chem. Phys.* **1944**, *12*, 125.
- [17] N. Ide, T. Fukuda, *Macromolecules* **1999**, *32*, 95.
- [18] Q. Liu, P. Zhang, M. Lu, *J. Polym. Sci. Part A: Polym. Chem.* **2005**, *43*, 2615.
- [19] C. Jiang, Y. Shen, S. Zhu, D. Hunkeler *J. Polym. Sci. Part A. Polym. Chem.* **2001**, *39*, 3780.
- [20] A. R. Wang, S. Zhu, *Polym. Eng. Sci.* **2005**, 720.
- [21] Q. Yu, J. Zhang, M. Cheng, S. Zhu, *Macromol. Chem. Phys.* **2006**, *207*, 287.
- [22] Q. Yu, M. Zhou, Y. Ding, B. Jiang, S. Zhu, *Polymer* **2007**, *48*, 7058.
- [23] G. Erdodi, J. P. Kennedy, *Prog. Polym. Sci.* **2006**, *31*, 1.
- [24] M. Trollsås, V. Y. Lee, D. Mecerreyes, P. Löwenheim, M. Möller, R. D. Miller, J. L. Hedrick, *Macromolecules* **2000**, *33*, 4619.
- [25] R. F. Storey, J. W. Sherman, *Macromolecules* **2002**, *35*, 1504.
- [26] A. Kowalski, A. Duda, S. Penszek, *Macromol. Rapid Commun.* **1998**, *19*, 567.
- [27] L. Mespouille, P. Degée, P. Dubois, *Eur. Polym. J.* **2005**, *41*, 1187.
- [28] P. J. Flory, *Principles of Polymer Chemistry*, Cornell University Press, Ithaca, NY, **1953**, p. 383.
- [29] H. W. Richtering, K. D. Gagnon, R. W. Lenz, R. C. Fuller, H. H. Winter, *Macromolecules* **1992**, *25*, 2429.
- [30] N. Ide, T. Fukuda, *Macromolecules* **1999**, *32*, 95.
- [31] S. H. Cho, M. S. Jhon, S. H. Yuk, *Eur. Polym. J.* **1999**, *35*, 1841.
- [32] X. Bories-Azeau, S. P. Armes, *Macromolecules* **2002**, *35*, 10241.
- [33] A. Charlesby, S. H. Pinner, *Proc. R. Soc. London, Ser. A* **1959**, *249*, 367.

Received: January 15, 2008
Published online: June 9, 2008